
Self-Attention as a Covariance Readout: A Unified View of In-Context Learning and Repetition

Haoren Xu
Fudan University
haorenxu25@m.fudan.edu.cn

Guanhua Fang
Fudan University
fanggh@fudan.edu.cn

Abstract

Large language models (LLMs) exhibit two striking and ostensibly unrelated behaviours: in-context learning (ICL) and repetitive generation. In both, the model behaves as though it had summarised the context into a population-level statistic and discarded token-level detail. We ask whether this “summarisation and forgetting” can be derived from the attention mechanism itself, and answer in the affirmative. Under stationary, ergodic and elliptical inputs, the softmax attention output converges almost surely to $\Theta_V \Sigma \Theta_K^\top \Theta_Q x_t$, where Σ is the input covariance; the long-context limit is therefore a linear readout of the input’s second-order statistics. Two consequences follow. (i) For in-context linear regression, a single softmax head can implement one step of population gradient descent. Stacking such heads with residual connections iterates this update and implements multiple gradient descent steps. (ii) Propagated across an L -layer transformer, this readout drives the terminal hidden state at the parametric $1/t$ rate to a deterministic function of the current token alone, so that autoregressive generation collapses asymptotically to a first-order Markov chain whose attracting orbits furnish a structural account of repetition and mode collapse. The two phenomena thus emerge as facets of a single covariance-readout principle.

1 Introduction

Modern large language models built on transformers [Vaswani et al., 2017] display behaviors that the architecture itself does not obviously predict. In-context learning (ICL) and repetitive generation have attracted particular attention.

When a pre-trained model is given a few input–output pairs in its prompt followed by a query input, it frequently produces outputs consistent with the demonstrated mapping, without any parameter update [Brown et al., 2020]. This raises the question of how the model extracts the mapping. Existing explanations include implicit gradient descent on the demonstrations [Von Oswald et al., 2023, Akyürek et al., 2022, Dai et al., 2023]; implicit Bayesian inference over a latent task variable [Xie et al., 2021, Wang et al., 2023]. A common thread across these interpretations is that the model reads part of its context into an internal regime—a latent distribution, rule, or task descriptor—that governs downstream predictions, while the specific identities of the demonstrations become secondary.

When the same models are sampled autoregressively, they are prone to fall into loops, producing near-verbatim repetitions of recent phrases, stylistic motifs, or topics [Holtzman et al., 2019, Welleck et al., 2019, Fu et al., 2021, Xu et al., 2022]. The model appears to settle into a persistent theme and fail to escape it; aggressive decoding schemes such as nucleus sampling [Holtzman et al., 2019] or objective modifications such as unlikelihood training [Welleck et al., 2019] mitigate but do not eliminate the effect. In the language of the preceding paragraph, the model behaves as if it has again inferred a regime—here, a persistent theme—and is unable to break out of it.

Though surface manifestations differ, both phenomena share a structural signature: the model extracts a regime from its context and then largely forgets which specific tokens induced that regime. In ICL, the regime is the latent input–output mapping implied by the demonstrations; the precise identities of the demonstrations are unimportant provided they pin down the mapping. In repetitive generation, the regime is a persistent theme or motif. In both cases, the model behaves as if it had summarized the context into a population-level statistic and discarded token-level detail. The central question of this paper is whether this “summarization and forgetting” can be derived from the attention mechanism itself.

We show that this summarization and forgetting is precisely what a softmax attention head performs. Under stationary, ergodic assumptions and weak-dependence conditions on the input process, the attention output converges to an exponentially tilted population mean that depends on the input only through its covariance. In the long-context limit, an attention head therefore acts as a covariance readout: a linear functional of the current token x_t whose matrix is determined jointly by the attention parameters $(\Theta_Q, \Theta_K, \Theta_V)$ and the input covariance Σ . Both ICL and repetitive generation follow from this single principle. For ICL, we exhibit a parameter choice, under which a single softmax head can implement one step of population gradient descent. Stacking such heads with residual connections iterates this update and implement multiple gradient descent steps. For repetition, we show that propagating this readout through L stacked layers produces, in the long-context limit, a deterministic position-wise map of the current token; autoregressive generation from such a composite is asymptotically a first-order Markov chain, whose attracting orbits provide a structural account of repetition and mode collapse.

Our contributions are as follows:

1. We derive closed-form directional limits under rotational and elliptical inputs, exposing the joint role of $(\Theta_Q, \Theta_K, \Theta_V)$ and Σ as a covariance readout. We prove a parametric $O(\tau_\alpha \text{tr}(\Sigma)/n) L^2$ concentration rate under sub-Gaussian strongly mixing inputs, quantifying $\text{tr}(\Sigma)$ as the effective cost of dimension.
2. We specialize the covariance-readout principle to in-context linear regression. A single head with distribution-determined projections realizes one step of population gradient descent, while a residual stack of such heads iterates this update across depth and progressively approaches the Bayes-optimal linear predictor.
3. We propagate the single-head result through depth and autoregressive decoding, obtaining a first-order Markov-chain limit for generation and connecting its attractor structure to repetition phenomena.

2 Related work

Theoretical analyses of ICL. A first strand of work treats ICL as learned optimization inside the forward pass. Von Oswald et al. [2023] and Akyürek et al. [2022] construct explicit transformer weights that implement one or more steps of gradient descent on the demonstration loss; Dai et al. [2023] frame the phenomenon as meta-optimization; Zhang et al. [2024] study the trained solutions rigorously in a linear setting. A second strand interprets ICL as implicit Bayesian inference over a latent task variable, with the prompt acting as evidence [Xie et al., 2021, Wang et al., 2023]. A third strand emphasizes mechanistic circuits: Olsson et al. [2022] identify induction heads as a token-level pattern-matching substrate, while Elhage et al. [2021] develop a compositional account of attention-based computation. Data-distributional accounts [Chan et al., 2022] situate ICL as an emergent property of training on distributions with burstiness and long-tailed structure. Our analysis occupies a complementary regime: we treat the attention head as a statistical estimator operating on a stationary ergodic input stream and exhibit a parameterization that implements gradient descent.

Repetition and degeneration. Repetition is a long-standing failure mode of neural text generation. Holtzman et al. [2019] analyze likelihood-maximizing decoding and propose nucleus sampling; Welleck et al. [2019] introduce unlikelihood training to explicitly penalize recently emitted tokens. Fu et al. [2021] provide a token-level explanation through a high-inflow phenomenon in the induced transition graph, and Xu et al. [2022] analyze repetition loops from a self-reinforcement perspective. These works operate at the decoding or token-statistics level and largely treat the underlying model as a black-box conditional distribution. Our Markov-closure result is complementary: we show that the

conditional distribution itself collapses, in the long-context limit, to a first-order kernel determined by a depth- L composition of covariance readouts, so that repetition and mode collapse become structural properties of the ergodic transformer, not artifacts of any particular sampler. This also reframes the high-inflow diagnosis of Fu et al. [2021]: tokens with many incoming transitions in the generated graph are those lying in the basin of attraction of the depth- L context-free map.

3 Theoretical Framework

3.1 Attention as a softmax barycenter

Notation. For nonzero u, v in a common Euclidean space, $\cos(u, v) := u^\top v / (\|u\| \|v\|)$. Vector norms are Euclidean and matrix norms are the corresponding operator norms.

Attention layer. Fix integers $d, d_k, d_v \geq 1$ for the input, key/query, and value dimensions. A causal single-head attention layer maps $(x_j)_{j \geq 1} \subset \mathbb{R}^d$ to outputs via parameters $\Theta_Q, \Theta_K \in \mathbb{R}^{d_k \times d}$ and $\Theta_V \in \mathbb{R}^{d_v \times d}$:

$$q_t = \Theta_Q x_t, \quad k_j = \Theta_K x_j, \quad v_j = \Theta_V x_j, \quad y_t = \sum_{j=1}^t a_{tj} v_j, \quad a_{tj} = \frac{e^{s_{tj}}}{\sum_{i \leq t} e^{s_{ti}}}, \quad s_{tj} = \frac{q_t^\top k_j}{\sqrt{d_k}}.$$

Barycenter factorization. Because $v_j = \Theta_V x_j$ is linear in x_j , the projection commutes with softmax weighting, giving

$$y_t = \Theta_V \bar{X}_t(q_t), \quad \bar{X}_t(q) := \frac{\sum_{j \leq t} x_j e^{q^\top \Theta_K x_j / \sqrt{d_k}}}{\sum_{i \leq t} e^{q^\top \Theta_K x_i / \sqrt{d_k}}}. \quad (1)$$

The attention output is thus the value projection of an exponentially tilted empirical mean of the inputs, with tilt governed by $q^\top \Theta_K x_j / \sqrt{d_k}$. Analysis of y_t reduces to analysis of the conditional mean $\bar{X}_t(q)$; once the direction of this mean is known, multiplication by Θ_V delivers the attention output.

Probabilistic framework. We model $(x_j)_{j \geq 1}$ as a random process on \mathbb{R}^d . For $q \neq 0$, set $p := \Theta_K^\top q$ and define

$$\bar{X}_n(q) := \frac{\sum_{j=1}^n x_j e^{p^\top x_j / \sqrt{d_k}}}{\sum_{i=1}^n e^{p^\top x_i / \sqrt{d_k}}}, \quad \Lambda(u) := \log \mathbb{E} e^{u^\top x_1} \text{ (wherever finite)}.$$

The identification of the ergodic limit depends only on the marginal law of x_1 ; rate statements depend additionally on the dependence structure.

The following elementary lemma, used repeatedly to convert L^2 errors into directional (cosine) errors, is proved in Appendix A.1.

Lemma 3.1 (Geometric stability). *Let $u \neq 0$ and $\|e\| \leq \eta \|u\|$ with $\eta \in [0, 1)$. Then $u + e \neq 0$ and $\cos(u + e, u) \geq \sqrt{1 - \eta^2}$.*

3.2 Ergodic alignment of the attention output

We now identify the long-context limit of y_t . The argument proceeds in three steps: an unconditional ergodic law, exact directional alignment under rotational input symmetry, and a joint-covariance readout under elliptical inputs.

3.2.1 Ergodic law of large numbers

Theorem 3.2 (Ergodic LLN). *Let $(x_j)_{j \geq 1}$ be stationary and ergodic on \mathbb{R}^d , and fix $q \neq 0$ with $p := \Theta_K^\top q$. Assume $\mathbb{E} e^{p^\top x_1 / \sqrt{d_k}} < \infty$ and $\mathbb{E}[\|x_1\| e^{p^\top x_1 / \sqrt{d_k}}] < \infty$. Then almost surely*

$$\bar{X}_n(q) \xrightarrow{\text{a.s.}} m_x(q) := \frac{\mathbb{E}[x_1 e^{p^\top x_1 / \sqrt{d_k}}]}{\mathbb{E}[e^{p^\top x_1 / \sqrt{d_k}}]}.$$

If moreover Λ is finite on a neighborhood of $p/\sqrt{d_k}$, then $m_x(q) = \nabla \Lambda(p/\sqrt{d_k})$.

Proof. Birkhoff's ergodic theorem, applied separately to the stationary ergodic, integrable sequences $(x_j e^{p^\top x_j / \sqrt{d_k}})_{j \geq 1}$ and $(e^{p^\top x_j / \sqrt{d_k}})_{j \geq 1}$, yields almost-sure convergence of the respective Cesàro averages to their expectations, the second of which is strictly positive. Taking the ratio gives the first claim. Differentiation under the integral sign, valid on the interior of the finiteness region of Λ , gives $\nabla \Lambda(u) = \mathbb{E}[x_1 e^{u^\top x_1}] / \mathbb{E}[e^{u^\top x_1}]$; setting $u = p / \sqrt{d_k}$ yields the second. \square

Since $y_t = \Theta_V \bar{X}_t(q_t)$ by (1), Theorem 3.2 lifts verbatim: $y_t \rightarrow \Theta_V m_x(q_t)$ almost surely. The remainder of this section is about identifying the direction of $m_x(q)$.

3.2.2 Exact alignment under rotational invariance

The simplest identifying structure is rotational invariance of the marginal input law.

Theorem 3.3 (Rotational-invariance alignment). *Assume the hypotheses of Theorem 3.2, $x_1 \neq 0$ almost surely, and $x_1 \stackrel{d}{=} R x_1$ for every $R \in O(d)$. Then for every $q \neq 0$ with $p := \Theta_K^\top q \neq 0$,*

$$m_x(q) = \gamma(\|p\|) \Theta_K^\top q, \quad \gamma(\|p\|) > 0,$$

and consequently $\cos(y_t, \Theta_V \Theta_K^\top \Theta_Q x_t) \xrightarrow{\text{a.s.}} 1$ whenever $\Theta_V \Theta_K^\top \Theta_Q x_t \neq 0$.

Proof. Define $T(p) := \mathbb{E}[x_1 e^{p^\top x_1 / \sqrt{d_k}}] / \mathbb{E}[e^{p^\top x_1 / \sqrt{d_k}}]$, so $m_x(q) = T(\Theta_K^\top q)$.

Direction. For every orthogonal $R \in O(d)$, rotational invariance gives, via the change of variable $x \mapsto Rx$,

$$T(p) = \mathbb{E}[R x_1 e^{p^\top R x_1 / \sqrt{d_k}}] / \mathbb{E}[e^{p^\top R x_1 / \sqrt{d_k}}] = R T(R^\top p),$$

so T is $O(d)$ -equivariant: $T(Rp) = R T(p)$. Taking R to fix p yields $T(p) = R T(p)$; hence $T(p) \in \text{span}\{p\}$, say $T(p) = \gamma_p p$. Equivariance then forces γ_p to depend only on $\|p\|$.

Positivity. Taking $R = -I$ yields $x_1 \stackrel{d}{=} -x_1$, so $Y := p^\top x_1$ is symmetric. Then

$$p^\top T(p) = \frac{\mathbb{E}[Y e^{Y / \sqrt{d_k}}]}{\mathbb{E}[e^{Y / \sqrt{d_k}}]} = \frac{\mathbb{E}[Y \sinh(Y / \sqrt{d_k})]}{\mathbb{E}[e^{Y / \sqrt{d_k}}]},$$

and $y \sinh(y / \sqrt{d_k}) \geq 0$ with equality only at $y = 0$. Rotational invariance and $x_1 \neq 0$ force the conditional law of $x_1 / \|x_1\|$ given $\{x_1 \neq 0\}$ to be uniform on S^{d-1} , so Y is not almost surely zero (since $p \neq 0$). Therefore $p^\top T(p) > 0$, i.e. $\gamma(\|p\|) > 0$.

Finally $y_t \rightarrow \Theta_V m_x(q_t) = \gamma(\|p_t\|) \Theta_V \Theta_K^\top \Theta_Q x_t$, and the positive scalar γ does not affect the cosine. \square

3.2.3 Joint-covariance limit under elliptical inputs

Relaxing rotational symmetry to ellipticity produces a covariance-rotated alignment.

Theorem 3.4 (Joint-covariance limit). *Assume the hypotheses of Theorem 3.2, and suppose $x_1 \stackrel{d}{=} BZ$ with $B \in \mathbb{R}^{d \times d}$ deterministic and invertible, $Z \neq 0$ rotationally invariant, and $\mathbb{E} e^{u^\top Z} < \infty$ on a neighborhood of $u = B^\top \Theta_K^\top q / \sqrt{d_k}$. Let $\Sigma := B B^\top \succ 0$. Then*

$$m_x(q) = \gamma_\Sigma(q) \Sigma \Theta_K^\top q, \quad \gamma_\Sigma(q) > 0,$$

where $\gamma_\Sigma(q)$ depends on B only through Σ and the quadratic form $q^\top \Theta_K \Sigma \Theta_K^\top q$. Consequently $y_t \xrightarrow{\text{a.s.}} \gamma_\Sigma(q_t) \Theta_V \Sigma \Theta_K^\top \Theta_Q x_t$, and the cosine with this target tends to 1 almost surely whenever the target is nonzero.

Proof. Set $p := \Theta_K^\top q$ and $w := B^\top p$. Since $p^\top x_1 \stackrel{d}{=} p^\top BZ = w^\top Z$,

$$m_x(q) = B \frac{\mathbb{E}[Z e^{w^\top Z / \sqrt{d_k}}]}{\mathbb{E}[e^{w^\top Z / \sqrt{d_k}}]}.$$

Theorem 3.3 applied to the rotationally invariant Z with “query” w gives the inner ratio as $\tilde{\gamma}(\|w\|) w$ with $\tilde{\gamma}(\|w\|) > 0$. Thus

$$m_x(q) = \tilde{\gamma}(\|w\|) BB^\top p = \tilde{\gamma}(\|w\|) \Sigma \Theta_K^\top q, \quad \gamma_\Sigma(q) := \tilde{\gamma}(\|B^\top \Theta_K^\top q\|) > 0.$$

Since $\|B^\top \Theta_K^\top q\|^2 = q^\top \Theta_K \Sigma \Theta_K^\top q$ depends on B only through Σ , so does $\gamma_\Sigma(q)$. Left-multiplying by Θ_V and using $y_t = \Theta_V \bar{X}_t(q_t) \rightarrow \Theta_V m_x(q_t)$ concludes. \square

Theorem 3.4 is the central structural result. In the long-context limit, the attention head is a linear function of x_t ,

$$y_t \approx \gamma_\Sigma(q_t) \underbrace{\Theta_V \Sigma \Theta_K^\top \Theta_Q}_{\text{covariance readout}} x_t,$$

whose matrix couples the attention parameters with the input second-order statistics. The realized context (x_1, \dots, x_{t-1}) enters only through the convergence: in the limit, the head forgets the identities of past tokens and retains only the population covariance Σ . Empirical results are given in Appendix B.1.

3.3 Finite-sample concentration under strong mixing

We now quantify the rate at which the covariance readout is attained. The scaling exposes $\text{tr}(\Sigma)$ as the effective cost of dimension and makes explicit the role of weak dependence through a single scalar.

Assumption 3.5 (Elliptical sub-Gaussian inputs with strong mixing). $(x_j)_{j \geq 1}$ is strictly stationary and ergodic on \mathbb{R}^d :

- (a) (Elliptical sub-Gaussian marginal) $x_1 \stackrel{d}{=} BZ$ with $B \in \mathbb{R}^{d \times d}$ deterministic and invertible, $\Sigma := BB^\top \succ 0$, Z rotationally invariant on \mathbb{R}^d with $\mathbb{E}Z = 0$, $\text{Cov}(Z) = I_d$, and $\mathbb{E}e^{u^\top Z} \leq e^{\sigma^2 \|u\|^2/2}$ for all $u \in \mathbb{R}^d$ and some $\sigma \geq 1$.
- (b) (Strong mixing) The Rosenblatt α -mixing coefficients satisfy $\tau_\alpha := 1 + 2 \sum_{k \geq 1} \sqrt{\alpha(k)} < \infty$.

Setting $\alpha \equiv 0$ recovers i.i.d. inputs with $\tau_\alpha = 1$; condition (b) is satisfied by geometrically ergodic Markov chains, hidden Markov models, and smooth causal functionals of such processes—the natural structural class for transformer hidden states.

Theorem 3.6 (Concentration of the covariance readout). *Under Assumption 3.5, for every $q \in \mathbb{R}^{d_k}$ with $q^\top \Theta_K \Sigma \Theta_K^\top q \leq d_k$ and every $n \geq 1$,*

$$\mathbb{E} \left\| \bar{X}_n(q) - m_x(q) \right\|^2 \leq C_1 \tau_\alpha \frac{\text{tr}(\Sigma)}{n}, \quad (2)$$

for a constant C_1 .

The proof is given in Appendix A.2.

Combining Theorem 3.6 with Theorem 3.4 and Lemma 3.1 yields a finite-sample alignment bound.

Corollary 3.7 (Finite-sample alignment). *Under Assumption 3.5, for any $(\Theta_Q, \Theta_K, \Theta_V)$ and x_t with $q_t := \Theta_Q x_t$ satisfying $q_t^\top \Theta_K \Sigma \Theta_K^\top q_t \leq d_k$ and $\Theta_V \Sigma \Theta_K^\top q_t \neq 0$,*

$$\mathbb{E} \left[1 - \cos(y_t, \Theta_V \Sigma \Theta_K^\top \Theta_Q x_t) \right] \leq \frac{C \tau_\alpha \|\Theta_V\|_{\text{op}}^2 \text{tr}(\Sigma)}{n \gamma_\Sigma(q_t)^2 \|\Theta_V \Sigma \Theta_K^\top q_t\|^2},$$

where C depends only on σ and $\gamma_\Sigma(q_t)$ is the positive scalar of Theorem 3.4.

4 In-context learning as a joint-covariance readout

Theorem 3.4 established that, under stationary ergodic elliptical inputs, the attention output y_t converges in direction to $\Theta_V \Sigma \Theta_K^\top \Theta_Q x_t$. We now specialise to the token structure used in in-context

learning (ICL), in which each input bundles a covariate and a target. The specialisation yields two observations. First, the simplest choice of projections realises, in the ergodic limit, a single step of population gradient descent on the in-context square loss: one self-attention layer is one GD step. Second, stacking such heads with residual connections iterates this update and converges to the Bayes-optimal in-context predictor: K self-attention layers are K GD steps. In-context learning of linear regression is therefore a direct consequence of the joint-covariance readout of Theorem 3.4.

4.1 The in-context prompt structure

Partition the input dimension as $d = d_u + d_w$ and write each token as

$$x_j = \begin{pmatrix} u_j \\ w_j \end{pmatrix} \in \mathbb{R}^d, \quad u_j \in \mathbb{R}^{d_u}, \quad w_j \in \mathbb{R}^{d_w},$$

where u_j is a covariate and w_j a (possibly masked) target. The selectors

$$S_u := [I_{d_u} \ 0] \in \mathbb{R}^{d_u \times d}, \quad S_w := [0 \ I_{d_w}] \in \mathbb{R}^{d_w \times d}$$

satisfy $S_u x = u$ and $S_w x = w$. Block the input covariance conformably,

$$\Sigma = \begin{pmatrix} \Sigma_{uu} & \Sigma_{uw} \\ \Sigma_{wu} & \Sigma_{ww} \end{pmatrix}, \quad \Sigma_{ab} := S_a \Sigma S_b^\top, \quad a, b \in \{u, w\}.$$

An ICL prompt presents $t - 1$ labelled examples followed by a query with masked label: $x_j = (u_j, w_j)^\top$ for $j < t$ and $x_t = (u_t, 0)^\top$. Under the canonical linear-regression task $w_j = \beta^\top u_j + \varepsilon_j$, $\varepsilon_j \perp u_j$, the Bayes/OLS regressor on u_t is

$$B^* u_t := \Sigma_{wu} \Sigma_{uu}^{-1} u_t,$$

the directional target of any learner that aspires to in-context linear regression.

4.2 A single head is one step of gradient descent

The simplest choice of projections for this prompt—key and query read the covariate slot, value reads the target slot—yields, directly from Theorem 3.4, a recognisable one-step Bayes estimator.

Corollary 4.1 (One-step Bayes readout). *Assume the hypotheses of Theorem 3.4 and choose*

$$\Theta_K = S_u, \quad \Theta_Q = S_u, \quad \Theta_V = S_w, \quad x_t = (u_t, 0)^\top.$$

Then, almost surely,

$$y_t \longrightarrow \gamma_{\Sigma}(q_t) \Sigma_{wu} u_t,$$

and $\cos(y_t, \Sigma_{wu} u_t) \xrightarrow{\text{a.s.}} 1$ whenever $\Sigma_{wu} u_t \neq 0$. If in addition (u_1, w_1) are jointly Gaussian with $w_1 = \beta^\top u_1 + \varepsilon$, $\varepsilon \perp u_1$, then $\Sigma_{wu} = \beta^\top \Sigma_{uu}$.

Proof. Substitute $\Theta_Q x_t = S_u x_t = u_t$ into Theorem 3.4:

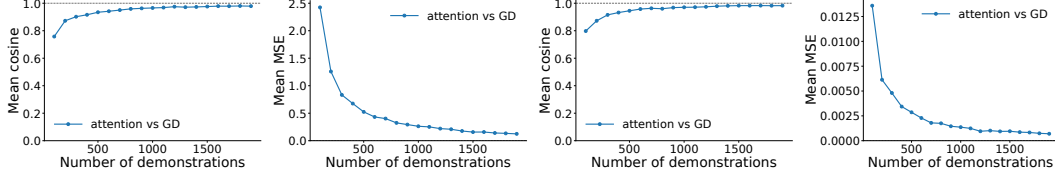
$$\Theta_V \Sigma \Theta_K^\top \Theta_Q x_t = S_w \Sigma S_u^\top u_t = \Sigma_{wu} u_t.$$

The final identity follows from the linear-model assumption. \square

Remark 4.2 (One layer = one step of population gradient descent). *Let $L(B) := \frac{1}{2} \mathbb{E} \|w - Bu\|^2$. Its gradient $\nabla L(B) = B \Sigma_{uu} - \Sigma_{wu}$ satisfies $\nabla L(0) = -\Sigma_{wu}$, so a single gradient-descent step from $B^{(0)} = 0$ with unit learning rate produces $\hat{B}^{(1)} u_t = \Sigma_{wu} u_t$ —exactly the directional readout of Corollary 4.1. A single softmax attention head therefore is a single step of population gradient descent for linear regression.*

4.3 Depth is multi-step gradient descent

The Bayes regressor $B^* u_t = \Sigma_{wu} \Sigma_{uu}^{-1} u_t$ differs from the one-step readout $\Sigma_{wu} u_t$ of Corollary 4.1 by the preconditioner Σ_{uu}^{-1} ; depth closes this gap under the following uniform long-context idealisation.



(a) Single head: cosine (b) Single head: MSE (c) Stacked heads: cosine (d) Stacked heads: MSE

Figure 1: Convergence of the joint-covariance readout for in-context linear regression. Panels (a)–(b) (Corollary 4.1): a single softmax head with selectors $\Theta_Q = \Theta_K = S_u$, $\Theta_V = S_w$, evaluated against the population one-step gradient-descent target $\Sigma_{wu}u_t$. Panels (c)–(d) (Proposition 4.4): an eight-layer residual stack of such heads with weights (3) and step size $\eta = 10^{-2}$, evaluated against the population eight-step iterate $B^{(K)}u_t$. The horizontal axis is the number of in-context demonstrations $t - 1$; panels (a) and (c) report the cosine similarity (dashed reference at 1, the ergodic limit predicted by Theorem 3.4), and panels (b) and (d) the mean squared error (dashed reference at 0). See Appendix B.2 for the full configuration.

Residual-stack construction. Hidden states $x_j^{(k)} = (u_j, r_j^{(k)}) \in \mathbb{R}^d$ are initialised with $r_j^{(0)} = w_j$ for $j < t$ and $r_t^{(0)} = 0$. Each of K blocks is instantiated with

$$\Theta_Q^{(k)} = \Theta_K^{(k)} = S_u, \quad \Theta_V^{(k)} = \eta S_w^\top S_w, \quad W_{\text{MLP}}^{(k)} = -S_w^\top S_w \in \mathbb{R}^{d \times d}, \quad (3)$$

i.e. queries and keys read the covariate slot, the value head produces the w -slot vector $\eta S_w^\top \sum_i \alpha_{ji}^{(k)} r_i^{(k)}$ with $\alpha_{ji}^{(k)} = \text{softmax}_i(u_j^\top u_i)$. Let $\xi_j^{(k)} \in \mathbb{R}^d$ denote the layer- k block output at position j in the stack. The block output and update are therefore

$$\xi_j^{(k)} = -\eta S_w^\top \sum_i \alpha_{ji}^{(k)} r_i^{(k)}, \quad x_j^{(k+1)} = x_j^{(k)} + \xi_j^{(k)}, \quad (4)$$

and $u_j^{(k+1)} = u_j$.

Induction across layers. Assume inductively $r_j^{(k)} = w_j - B^{(k)}u_j$ for every $j \geq 1$ (with the convention $w_t := 0$), whence the cross-covariance between the residual slot and the covariate satisfies

$$\text{Cov}(r^{(k)}, u) = \Sigma_{wu} - B^{(k)}\Sigma_{uu} = -\nabla L(B^{(k)}).$$

with $L(B) := \frac{1}{2}\mathbb{E}\|w - Bu\|^2$, $\nabla L(B) = B\Sigma_{uu} - \Sigma_{wu}$, and $B^{(k+1)} = B^{(k)} - \eta \nabla L(B^{(k)})$, $B^{(0)} = 0$. Applying Theorem 3.4 to the layer- k hidden-state process with query $q_j^{(k)} = \Theta_Q^{(k)}x_j^{(k)} = u_j$, the softmax-weighted average in (4) converges, in the long-context limit, to

$$S_w \xi_j^{(k)} = -\eta \sum_i \alpha_{ji}^{(k)} r_i^{(k)} \longrightarrow -\eta \gamma_\Sigma^{(k)} \text{Cov}(r^{(k)}, u) u_j = \eta_k \nabla L(B^{(k)}) u_j,$$

where $\gamma_\Sigma^{(k)} > 0$ is the positive directional scalar supplied by Theorem 3.4 at layer k , and we have introduced the effective layer- k step size

$$\eta_k := \eta \gamma_\Sigma^{(k)} > 0.$$

Thus η_k is the nominal step size η of (3) rescaled by the Theorem 3.4 scalar $\gamma_\Sigma^{(k)}$.

Assumption 4.3 (Uniform long-context approximation). Let $\xi_j^{(k)} \in \mathbb{R}^d$ denote the layer- k block output at position j in the stack. For every $k \geq 0$ and every $j \geq 1$,

$$S_w \xi_j^{(k)} \approx \eta_k \nabla L(B^{(k)}) u_j, \quad (5)$$

Corollary 3.7 establishes (5) at position j with L^2 -error $O((\tau_\alpha \text{tr } \Sigma / j)^{1/2})$; Assumption 4.3 extends it uniformly in j .

Assumption 4.3 asserts the above approximation uniformly in j , so that η_k may be treated as a single scalar per layer (in the Gaussian special case it reduces to $\eta_k = \eta/\sqrt{d_u}$ exactly, constant across layers). Substituting into the block update (4) gives

$$r_j^{(k+1)} = r_j^{(k)} + S_w \xi_j^{(k)} \approx (w_j - B^{(k)} u_j) + \eta_k \nabla L(B^{(k)}) u_j = w_j - B^{(k+1)} u_j,$$

with $B^{(k+1)} := B^{(k)} - \eta_k \nabla L(B^{(k)})$. This is the inductive hypothesis at layer $k + 1$; the base case $k = 0$ follows from the initialisation.

Proposition 4.4 (K layers $\approx K$ gradient-descent steps). *Under Theorem 3.4 and Assumption 4.3, with $0 < \eta_k < 2/\lambda_{\max}(\Sigma_{uu})$, the query prediction $\hat{w}_t^{(K)} := -r_t^{(K)}$ satisfies*

$$\hat{w}_t^{(K)} \xrightarrow[t \rightarrow \infty]{\text{a.s.}} B^{(K)} u_t$$

We empirically verify the two structural claims of Sections 4.2–4.3: that a single softmax head with the selectors of Corollary 4.1 realises one step of population gradient descent on the in-context square loss, and that the residual stack of Section 4.3 iterates that update across depth. For each prompt we sample a fresh task (Σ_{uu}, β) , generate $t - 1$ Gaussian covariates with noiseless targets $w_j = \beta^\top u_j$, and feed the resulting prompt through the parameter-frozen heads of (3); we then compare the head output against its theoretical population target— $\Sigma_{wu} u_t$ for the single layer and the K -step iterate $B^{(K)} u_t$ for the stack—using both cosine similarity and mean squared error, averaged over hundreds of independently sampled tasks per prompt-length value. Figure 1 summarises the outcome: cosine similarities approach unity and squared errors decay toward zero as the prompt grows. The match is essentially exact already at a few hundred demonstrations, supporting the interpretation of stacked attention as gradient descent on the in-context loss.

5 Multi-layer collapse and Markovian repetition

We now propagate the single-head covariance readout through depth and through autoregressive decoding. The results say that the terminal hidden state of an L -layer transformer becomes, in the long-context limit, a deterministic position-wise map of the current token alone, and that autoregressive generation therefore collapses asymptotically into a first-order Markov chain.

Multi-layer setup. Fix depth $L \geq 1$ with single-head causal attention at each layer and parameters $\{(\Theta_Q^{(\ell)}, \Theta_K^{(\ell)}, \Theta_V^{(\ell)})\}_{\ell=1}^L$; take $d_v = d$ for notational clarity.¹ Setting $h_j^{(0)} := x_j$, the hidden-state recursion is

$$q_j^{(\ell)} = \Theta_Q^{(\ell)} h_j^{(\ell-1)}, \quad y_j^{(\ell)} = \Theta_V^{(\ell)} \bar{X}_j^{(\ell)}(q_j^{(\ell)}), \quad h_j^{(\ell)} = \Phi^{(\ell)}(h_j^{(\ell-1)}, y_j^{(\ell)}),$$

where $\bar{X}_j^{(\ell)}$ is the softmax barycenter (1) applied to $(h_i^{(\ell-1)})_{i \leq j}$ and $\Phi^{(\ell)} : \mathbb{R}^d \times \mathbb{R}^d \rightarrow \mathbb{R}^d$ is a globally L_Φ -Lipschitz residual block (covering pre-norm updates and Lipschitz MLPs).

Assumption 5.1 (Equilibrium regime). $(x_j)_{j \in \mathbb{Z}}$ satisfies Assumption 3.5. For each $\ell \in \{0, \dots, L-1\}$, the hidden-state process $(h_j^{(\ell)})_{j \in \mathbb{Z}}$ satisfies Assumption 3.5 with covariance $\Sigma_\ell \succ 0$ and mixing constant $\tau_\alpha^{(\ell)} < \infty$.

Context-free layer maps. Define $F^{(0)} := \text{id}$ and recursively, for $\ell = 1, \dots, L$,

$$F^{(\ell)}(x) := \Phi^{(\ell)}(F^{(\ell-1)}(x), r^{(\ell)} \circ F^{(\ell-1)}(x)), \quad r^{(\ell)}(h) := \gamma_{\Sigma_{\ell-1}}(\Theta_Q^{(\ell)} h) \Theta_V^{(\ell)} \Sigma_{\ell-1} (\Theta_K^{(\ell)})^\top \Theta_Q^{(\ell)} h. \quad (6)$$

Each $F^{(\ell)}$ is a deterministic, position-wise function of its argument: it depends on process history only through the population covariances $\Sigma_0, \dots, \Sigma_{\ell-1}$, which are shift-invariant.

Theorem 5.2 (Multi-layer context forgetting). *Under Assumption 5.1 and $(q_t^{(\ell)})^\top \Theta_K^{(\ell)} \Sigma_{\ell-1} (\Theta_K^{(\ell)})^\top q_t^{(\ell)} \leq d_k$ for each ℓ ,*

$$h_t^{(L)} - F^{(L)}(x_t) \xrightarrow[t \rightarrow \infty]{\text{a.s.}} 0 \quad \text{as} \quad t \rightarrow \infty,$$

¹The extension to H -head attention is immediate: each head admits its own context-free readout and the output projection applied to the concatenation yields a composite readout to which the induction of Theorem 5.2 applies verbatim.

and for every $t \geq 1$,

$$\mathbb{E} \left\| h_t^{(L)} - F^{(L)}(x_t) \right\|^2 \leq \frac{C_L T_L}{t}, \quad T_L := \sum_{\ell=0}^{L-1} \tau_\alpha^{(\ell)} \text{tr}(\Sigma_\ell), \quad (7)$$

with C_L depending only on σ , L_Φ , and the operator norms $\{\|\Theta^{(\ell)}\|_{\text{op}}\}_{\ell \leq L}$.

The proof is given in Appendix A.3.

Autoregressive decoding. Decoding from a depth- L model samples the next token according to a Lipschitz rule applied to the terminal hidden state,

$$x_{t+1} = \Psi(h_t^{(L)}, x_t, \xi_{t+1}), \quad (\xi_t)_{t \geq 1} \text{ i.i.d.}, \quad \xi_{t+1} \perp \mathcal{H}_t^{(L)}, \quad (8)$$

with Ψ L_Ψ -Lipschitz in its first argument uniformly in the others. Equation (8) covers the composition of an LM head with a softmax/greedy/temperature/top- k /nucleus sampler and a token re-embedding map.

Proposition 5.3 (Markov closure). *Under Assumption 5.1 and dynamics (8),*

$$\left\| x_{t+1} - \Psi(F^{(L)}(x_t), x_t, \xi_{t+1}) \right\| \xrightarrow{\text{a.s.}} 0 \quad \text{as} \quad t \rightarrow \infty.$$

Consequently, for every bounded Lipschitz $\varphi : \mathbb{R}^d \rightarrow \mathbb{R}$,

$$\mathbb{E}[\varphi(x_{t+1}) \mid \mathcal{H}_t] - K\varphi(x_t) \xrightarrow{\text{a.s.}} 0, \quad K\varphi(x) := \mathbb{E}_\xi[\varphi(\Psi(F^{(L)}(x), x, \xi))],$$

so the generated process is asymptotically a time-homogeneous first-order Markov chain with transition kernel $K = K[\{\Theta^{(\ell)}\}, \{\Sigma_\ell\}, \Psi]$.

Proof. Lipschitzness of Ψ in its first argument and Theorem 5.2 give the first displayed convergence. The conditional-expectation identity follows from bounded convergence and $\xi_{t+1} \perp \mathcal{H}_t^{(L)}$. The detailed proof is given in Appendix A.4. \square

Proposition 5.3 is our main structural claim for repetition. A multi-layer transformer generates from a first-order Markov kernel in the long-context limit, regardless of depth. Depth increases the expressivity of the kernel— $F^{(L)}$ is a composition of L low-rank context-free readouts interleaved with Lipschitz residuals and can represent rich nonlinear dynamics—but cannot make the generated process anything other than first-order Markov. Within this picture, repetition corresponds to attracting fixed points or short cycles of K : if $F^{(L)}$ has an attracting fixed point x^* at which $\Psi(F^{(L)}(x^*), x^*, \xi)$ concentrates near x^* , generation converges to x^* and produces token-level loops; attracting cycles yield periodic motifs. This view offers a dynamical reading of the high-inflow phenomenon identified by Fu et al. [2021]: tokens with many incoming transitions in the generated graph are precisely those in the basin of attraction of $F^{(L)}$.

6 Conclusion

We have argued that a single principle—softmax attention as a covariance readout—organizes two seemingly distinct phenomena in large language models. In-context learning (for linear regression) arises when a single head’s covariance readout aligns with a task-relevant second-order statistic of the data. Repetitive generation arises when the same readout is propagated through depth: the model’s conditional distribution collapses in the long-context limit to a first-order Markov chain whose attracting orbits manifest as repeated text. Both phenomena reflect the same mechanism of regime inference with context forgetting.

Scope and limitations. Our analysis is asymptotic in the context length and assumes stationarity, ergodicity, and weak dependence of the input process; real prompts could be non-stationary, especially across conversational turns, and out-of-distribution contexts escape the equilibrium regime. The elliptical sub-Gaussian marginal is a modelling assumption that is consistent with empirical observations on normalized hidden states but is not derived from first principles. The ICL result establishes Bayes-optimal alignment for linear regression, not for arbitrary task classes.

References

- Ekin Akyürek, Dale Schuurmans, Jacob Andreas, Tengyu Ma, and Denny Zhou. What learning algorithm is in-context learning? investigations with linear models. *arXiv preprint arXiv:2211.15661*, 2022.
- Tom Brown, Benjamin Mann, Nick Ryder, Melanie Subbiah, Jared D Kaplan, Prafulla Dhariwal, Arvind Neelakantan, Pranav Shyam, Girish Sastry, Amanda Askell, et al. Language models are few-shot learners. *Advances in neural information processing systems*, 33:1877–1901, 2020.
- Stephanie Chan, Adam Santoro, Andrew Lampinen, Jane Wang, Aaditya Singh, Pierre Richemond, James McClelland, and Felix Hill. Data distributional properties drive emergent in-context learning in transformers. *Advances in neural information processing systems*, 35:18878–18891, 2022.
- Damai Dai, Yutao Sun, Li Dong, Yaru Hao, Shuming Ma, Zhifang Sui, and Furu Wei. Why can gpt learn in-context? language models secretly perform gradient descent as meta-optimizers. In *Findings of the Association for Computational Linguistics: ACL 2023*, pages 4005–4019, 2023.
- Nelson Elhage, Neel Nanda, Catherine Olsson, Tom Henighan, Nicholas Joseph, Ben Mann, Amanda Askell, Yuntao Bai, Anna Chen, Tom Conerly, et al. A mathematical framework for transformer circuits. *Transformer Circuits Thread*, 1(1):12, 2021.
- Zihao Fu, Wai Lam, Anthony Man-Cho So, and Bei Shi. A theoretical analysis of the repetition problem in text generation, 2021. URL <https://arxiv.org/abs/2012.14660>.
- Ari Holtzman, Jan Buys, Li Du, Maxwell Forbes, and Yejin Choi. The curious case of neural text degeneration. *arXiv preprint arXiv:1904.09751*, 2019.
- Catherine Olsson, Nelson Elhage, Neel Nanda, Nicholas Joseph, Nova DasSarma, Tom Henighan, Ben Mann, Amanda Askell, Yuntao Bai, Anna Chen, et al. In-context learning and induction heads. *arXiv preprint arXiv:2209.11895*, 2022.
- Emmanuel Rio et al. *Asymptotic theory of weakly dependent random processes*, volume 80. Springer, 2017.
- Ashish Vaswani, Noam Shazeer, Niki Parmar, Jakob Uszkoreit, Llion Jones, Aidan N Gomez, Łukasz Kaiser, and Illia Polosukhin. Attention is all you need. *Advances in neural information processing systems*, 30, 2017.
- Johannes Von Oswald, Eyvind Niklasson, Ettore Randazzo, João Sacramento, Alexander Mordvintsev, Andrey Zhmoginov, and Max Vladymyrov. Transformers learn in-context by gradient descent. In *International Conference on Machine Learning*, pages 35151–35174. PMLR, 2023.
- Xinyi Wang, Wanrong Zhu, Michael Saxon, Mark Steyvers, and William Yang Wang. Large language models are latent variable models: Explaining and finding good demonstrations for in-context learning. *Advances in Neural Information Processing Systems*, 36:15614–15638, 2023.
- Sean Welleck, Ilia Kulikov, Stephen Roller, Emily Dinan, Kyunghyun Cho, and Jason Weston. Neural text generation with unlikelihood training. *arXiv preprint arXiv:1908.04319*, 2019.
- Sang Michael Xie, Aditi Raghunathan, Percy Liang, and Tengyu Ma. An explanation of in-context learning as implicit bayesian inference. *arXiv preprint arXiv:2111.02080*, 2021.
- Jin Xu, Xiaojiang Liu, Jianhao Yan, Deng Cai, Huayang Li, and Jian Li. Learning to break the loop: Analyzing and mitigating repetitions for neural text generation. *Advances in Neural Information Processing Systems*, 35:3082–3095, 2022.
- Ruiqi Zhang, Spencer Frei, and Peter L Bartlett. Trained transformers learn linear models in-context. *Journal of Machine Learning Research*, 25(49):1–55, 2024.

Appendix of ‘‘Self-Attention as a Covariance Readout’’

A Proofs

A.1 Proof of Lemma 3.1

Proof of Lemma 3.1. Set $s := u + e$. By the triangle inequality $\|s\| \geq \|u\| - \|e\| \geq (1 - \eta)\|u\| > 0$, so $s \neq 0$. Expand $\|s\|^2 = \|u\|^2 + 2u^\top e + \|e\|^2$; combined with $u^\top s = \|u\|^2 + u^\top e$ and $|u^\top e| \leq \|u\| \|e\|$,

$$\cos(s, u) = \frac{u^\top s}{\|u\| \|s\|} = \frac{\|u\| + u^\top e / \|u\|}{\|s\|} \geq \frac{\|u\| - \|e\|}{\|s\|}.$$

Hence $\cos(s, u)^2 \geq (\|u\| - \|e\|)^2 / \|s\|^2$; expanding and using $|u^\top e| \leq \|u\| \|e\|$ yields $\cos(s, u)^2 \geq 1 - (\|e\| / \|u\|)^2 \geq 1 - \eta^2$, i.e. $\cos(s, u) \geq \sqrt{1 - \eta^2}$. \square

A.2 Proof of Theorem 3.6

The following tilted-moment estimate is used throughout the proof.

Lemma A.1 (Tilted second moment). *Under Assumption 3.5(a), for every $q \in \mathbb{R}^{d_k}$ with $q^\top \Theta_K \Sigma \Theta_K^\top q \leq d_k$ and $p := \Theta_K^\top q$,*

$$\mathbb{E} \left[\|x_1\|^2 e^{2p^\top x_1 / \sqrt{d_k}} \right] \leq C(\sigma) \operatorname{tr}(\Sigma).$$

Proof. Let $C(\sigma)$ be a positive constant depending only on σ whose value may change from line to line. Fix $q \in \mathbb{R}^{d_k}$ with $q^\top \Theta_K \Sigma \Theta_K^\top q \leq d_k$ and set

$$p := \Theta_K^\top q, \quad w := B^\top p.$$

Because $\|w\|^2 = p^\top B B^\top p = p^\top \Sigma p = q^\top \Theta_K \Sigma \Theta_K^\top q \leq d_k$, we have

$$\|w\|^2 / d_k \leq 1. \tag{9}$$

The elliptical representation $x_1 \stackrel{d}{=} BZ$ yields $p^\top x_1 \stackrel{d}{=} w^\top Z$. Fix an orthonormal basis $\{e_i\}_{i=1}^d$ of \mathbb{R}^d . Expanding $\|x_1\|^2 = \sum_i (e_i^\top x_1)^2$ and applying Cauchy–Schwarz term-by-term,

$$\mathbb{E} \left[\|x_1\|^2 e^{2p^\top x_1 / \sqrt{d_k}} \right] \leq \sum_{i=1}^d (\mathbb{E} (e_i^\top x_1)^4)^{1/2} (\mathbb{E} e^{4p^\top x_1 / \sqrt{d_k}})^{1/2}. \tag{10}$$

By the sub-Gaussian MGF of Z and (9),

$$\mathbb{E} e^{4p^\top x_1 / \sqrt{d_k}} = \mathbb{E} e^{(4w / \sqrt{d_k})^\top Z} \leq e^{8\sigma^2 \|w\|^2 / d_k} \leq e^{8\sigma^2}. \tag{11}$$

For every $v \in \mathbb{R}^d$, $\mathbb{E} e^{v^\top x_1} = \mathbb{E} e^{(B^\top v)^\top Z} \leq \exp(\sigma^2 v^\top \Sigma v / 2)$, so x_1 is sub-Gaussian with proxy covariance $\sigma^2 \Sigma$. In particular, each scalar $e_i^\top x_1$ is sub-Gaussian with parameter $\sigma \sqrt{e_i^\top \Sigma e_i}$, hence

$$\mathbb{E} (e_i^\top x_1)^4 \leq C \sigma^4 (e_i^\top \Sigma e_i)^2. \tag{12}$$

Combining (11) and (12) in (10) and using $\sum_i e_i^\top \Sigma e_i = \operatorname{tr}(\Sigma)$,

$$\mathbb{E} \left[\|x_1\|^2 e^{2p^\top x_1 / \sqrt{d_k}} \right] \leq C(\sigma) \sum_{i=1}^d (e_i^\top \Sigma e_i) = C(\sigma) \operatorname{tr}(\Sigma). \quad \square$$

Proof of Theorem 3.6. Let $C(\sigma)$ denote a positive constant depending only on σ whose value may change between occurrences, and let C denote an absolute constant.

Setup and notation. Fix $q \in \mathbb{R}^{d_k}$ with $q^\top \Theta_K \Sigma \Theta_K^\top q \leq d_k$ and set

$$p := \Theta_K^\top q, \quad w := B^\top p.$$

Because $\|w\|^2 = p^\top B B^\top p = p^\top \Sigma p = q^\top \Theta_K \Sigma \Theta_K^\top q \leq d_k$, we have

$$\|w\|^2/d_k \leq 1. \quad (13)$$

The elliptical representation $x_1 \stackrel{d}{=} BZ$ yields $p^\top x_1 \stackrel{d}{=} w^\top Z$. Define

$$\zeta_j := e^{p^\top x_j / \sqrt{d_k}}, \quad \bar{\zeta} := \mathbb{E}\zeta_1, \quad m := m_x(q) = \frac{\mathbb{E}[x_1 \zeta_1]}{\bar{\zeta}},$$

and the empirical quantities

$$N_n := \frac{1}{n} \sum_{j=1}^n x_j \zeta_j, \quad D_n := \frac{1}{n} \sum_{j=1}^n \zeta_j, \quad R_n := N_n - m D_n = \frac{1}{n} \sum_{j=1}^n (x_j - m) \zeta_j.$$

Then $\bar{X}_n(q) = N_n/D_n$, $\mathbb{E}N_n = m\bar{\zeta}$, $\mathbb{E}D_n = \bar{\zeta}$, $\mathbb{E}R_n = 0$, and the exact identity

$$\bar{X}_n(q) - m = \frac{R_n}{D_n} = \frac{N_n - m\bar{\zeta}}{D_n} - m \frac{D_n - \bar{\zeta}}{D_n}. \quad (14)$$

Step 1: Moment estimates.

(1a) *Exponential moments of ζ_1 .* By Assumption 3.5(a) and (13), for every $r \in \mathbb{R}$,

$$\mathbb{E}\zeta_1^r = \mathbb{E} \exp\left(\frac{r w^\top Z}{\sqrt{d_k}}\right) \leq \exp\left(\frac{\sigma^2 r^2 \|w\|^2}{2d_k}\right) \leq e^{\sigma^2 r^2 / 2}. \quad (15)$$

Hence $\|\zeta_1\|_{L^r} \leq e^{\sigma^2 r / 2}$, and $\zeta_1 \in L^r$ for every $r < \infty$.

(1b) *Lower bound on $\bar{\zeta}$.* Jensen's inequality applied to $z \mapsto e^z$, together with $\mathbb{E}[p^\top x_1] = p^\top \mathbb{E}x_1 = 0$, gives

$$\bar{\zeta} \geq e^{\mathbb{E}[p^\top x_1] / \sqrt{d_k}} = 1. \quad (16)$$

(1c) *Tilted L^4 bound.* Since $x_1 = BZ$ with Z sub-Gaussian of parameter σ , x_1 is sub-Gaussian with proxy $\sigma^2 \Sigma$: for every unit $u \in \mathbb{R}^d$ and integer $k \geq 1$, $\mathbb{E}(u^\top x_1)^{2k} \leq C_k \sigma^{2k} (u^\top \Sigma u)^k$. Cauchy-Schwarz combined with (15) yields

$$\begin{aligned} \|u^\top x_1 \zeta_1\|_{L^4}^4 &= \mathbb{E}(u^\top x_1)^4 \zeta_1^4 \leq (\mathbb{E}(u^\top x_1)^8)^{1/2} (\mathbb{E}\zeta_1^8)^{1/2} \\ &\leq (C_4 \sigma^8 (u^\top \Sigma u)^4)^{1/2} \cdot e^{16\sigma^2} \leq C(\sigma) (u^\top \Sigma u)^2, \end{aligned}$$

whence

$$\|u^\top x_1 \zeta_1\|_{L^4}^2 \leq C(\sigma) u^\top \Sigma u. \quad (17)$$

The same argument with no factor of x_1 shows $\|\zeta_1\|_{L^4}^2 \leq e^{2\sigma^2} \leq C(\sigma)$.

(1d) *Bound on $\|m\|$.* By Jensen and Lemma A.1,

$$\|m\| \leq \frac{\mathbb{E}\|x_1 \zeta_1\|}{\bar{\zeta}} \leq \frac{(\mathbb{E}\|x_1\|^2 \zeta_1^2)^{1/2}}{\bar{\zeta}} \leq (C(\sigma) \text{tr}(\Sigma))^{1/2},$$

using $\bar{\zeta} \geq 1$ from (16). Thus

$$\|m\|^2 \leq C(\sigma) \text{tr}(\Sigma). \quad (18)$$

Step 2: L^2 -rates via Rio's covariance inequality. For a stationary absolutely regular sequence $(Y_j)_{j \in \mathbb{Z}}$ with $Y_0 \in L^4$, we use Rio's covariance inequality in its strong-mixing form. Let $\alpha(h)$ denote the strong-mixing coefficient between $\sigma(Y_j : j \leq 0)$ and $\sigma(Y_j : j \geq h)$. Rio's covariance inequality [Rio et al., 2017, Eq. (1.12b)] implies, by taking $q = r = 4$ and $p = 2$,

$$|\text{Cov}(Y_0, Y_h)| \leq 2 \sqrt{\alpha(h)} \|Y_0\|_{L^4} \|Y_h\|_{L^4}.$$

By stationarity, $\|Y_h\|_{L^4} = \|Y_0\|_{L^4}$, hence

$$|\text{Cov}(Y_0, Y_h)| \leq 2 \sqrt{\alpha(h)} \|Y_0\|_{L^4}^2, \quad h \geq 1. \quad (19)$$

Fix a unit vector $u \in \mathbb{R}^d$ and apply (19) to $Y_j := u^\top x_j \zeta_j$ (stationary by Assumption 3.5), whose L^4 -norm is controlled by (17). Expanding the variance of the partial sum and using stationarity:

$$\begin{aligned} \text{Var}(u^\top N_n) &= \frac{\text{Var}(Y_0)}{n} + \frac{2}{n^2} \sum_{h=1}^{n-1} (n-h) \text{Cov}(Y_0, Y_h) \\ &\leq \frac{\|Y_0\|_{L^4}^2}{n} + \frac{2\|Y_0\|_{L^4}^2}{n} \sum_{h=1}^{n-1} C\sqrt{\alpha(h)} \\ &\leq \frac{C\|Y_0\|_{L^4}^2}{n} \left(1 + 2 \sum_{h=1}^{\infty} \sqrt{\alpha(h)}\right) = \frac{C\tau_\alpha \|Y_0\|_{L^4}^2}{n} \leq \frac{C(\sigma)\tau_\alpha u^\top \Sigma u}{n}, \end{aligned}$$

where $\text{Var}(Y_0) \leq \|Y_0\|_{L^4}^2$. Summing over an orthonormal basis $\{e_i\}_{i=1}^d$ of \mathbb{R}^d converts this scalar bound into a trace bound:

$$\mathbb{E}\|N_n - m\bar{\zeta}\|^2 = \sum_{i=1}^d \text{Var}(e_i^\top N_n) \leq \frac{C(\sigma)\tau_\alpha \text{tr}(\Sigma)}{n}. \quad (20)$$

Applying the same argument to the scalar $Y_j = \zeta_j$ and using $\|\zeta_0\|_{L^4}^2 \leq e^{2\sigma^2}$:

$$\mathbb{E}(D_n - \bar{\zeta})^2 = \text{Var}(D_n) \leq \frac{C(\sigma)\tau_\alpha}{n}. \quad (21)$$

Step 3: Control of D_n from below. Set $A_n := \{D_n > \bar{\zeta}/2\}$. By Chebyshev, (21), and $\bar{\zeta} \geq 1$,

$$\mathbb{P}(A_n^c) \leq \mathbb{P}(|D_n - \bar{\zeta}| \geq \bar{\zeta}/2) \leq \frac{4\mathbb{E}(D_n - \bar{\zeta})^2}{\bar{\zeta}^2} \leq \frac{C(\sigma)\tau_\alpha}{n}. \quad (22)$$

For the sharper tail needed in Step 5, it suffices to control the fourth moment of the centered denominator. Set

$$Y_j := \zeta_j - \bar{\zeta}, \quad S_n := \sum_{j=1}^n Y_j.$$

Rio's fourth-moment bound for strongly mixing sequences [Rio et al., 2017, Eq. (2.11)] gives

$$\mathbb{E}S_n^4 \leq 768n^2 \left(\sum_{m=0}^{n-1} \sqrt{\alpha_m} \right)^2.$$

Therefore

$$\mathbb{E}|S_n|^4 \leq C(\alpha)n^2.$$

Because $D_n - \bar{\zeta} = n^{-1}S_n$,

$$\mathbb{E}|D_n - \bar{\zeta}|^4 \leq \frac{C(\alpha)}{n^2}.$$

Consequently, by Markov's inequality and $\bar{\zeta} \geq 1$,

$$\mathbb{P}(A_n^c) \leq \mathbb{P}\left(|D_n - \bar{\zeta}| \geq \frac{\bar{\zeta}}{2}\right) \leq \frac{16\mathbb{E}|D_n - \bar{\zeta}|^4}{\bar{\zeta}^4} \leq \frac{C(\alpha)}{n^2}.$$

Step 4: Ratio argument on the good event A_n . From (14) and the decomposition $R_n = (N_n - m\bar{\zeta}) - m(D_n - \bar{\zeta})$, the triangle inequality and $D_n \geq \bar{\zeta}/2 \geq 1/2$ on A_n give

$$\|\bar{X}_n - m\| \mathbf{1}_{A_n} \leq \frac{2}{\bar{\zeta}} (\|N_n - m\bar{\zeta}\| + \|m\| |D_n - \bar{\zeta}|) \mathbf{1}_{A_n} \leq 2(\|N_n - m\bar{\zeta}\| + \|m\| |D_n - \bar{\zeta}|).$$

Squaring, taking expectations, and combining (20), (21), (18):

$$\begin{aligned} \mathbb{E}\|\bar{X}_n - m\|^2 \mathbf{1}_{A_n} &\leq 8\mathbb{E}\|N_n - m\bar{\zeta}\|^2 + 8\|m\|^2 \mathbb{E}(D_n - \bar{\zeta})^2 \\ &\leq 8 \frac{C(\sigma)\tau_\alpha \text{tr}(\Sigma)}{n} + 8C(\sigma) \text{tr}(\Sigma) \cdot \frac{C(\sigma)\tau_\alpha}{n} \leq \frac{C(\sigma)\tau_\alpha \text{tr}(\Sigma)}{n}. \end{aligned} \quad (23)$$

Step 5: Absorption of the exceptional event A_n^c . On A_n^c the denominator D_n admits no sample-path lower bound, so $\|\bar{X}_n\|$ must be controlled in expectation. We combine Hölder's inequality with a uniform L^6 -moment bound on \bar{X}_n .

(5a) *Uniform L^6 bound on \bar{X}_n .* Setting $a_j := \zeta_j / \sum_{i=1}^n \zeta_i \in [0, 1]$, we have $\bar{X}_n = \sum_{j=1}^n a_j x_j$ with $\sum_j a_j = 1$. Convexity of $x \mapsto \|x\|^6$ on \mathbb{R}^d gives

$$\|\bar{X}_n\|^6 \leq \sum_{j=1}^n a_j \|x_j\|^6 \leq \max_{j \leq n} \|x_j\|^6,$$

hence, by stationarity,

$$\mathbb{E}\|\bar{X}_n\|^6 \leq \mathbb{E} \max_{j \leq n} \|x_j\|^6 \leq \sum_{j=1}^n \mathbb{E}\|x_j\|^6 = n \mathbb{E}\|x_1\|^6.$$

Decomposing $\|x_1\|^2 = \sum_{i=1}^d (e_i^\top x_1)^2$ in an orthonormal basis $\{e_i\}_{i=1}^d$ of \mathbb{R}^d , applying Minkowski's inequality in L^3 , and invoking the scalar sub-Gaussian moment bound $\|e_i^\top x_1\|_{L^6}^2 \leq C(\sigma) e_i^\top \Sigma e_i$ (Step 1(c) with $k = 3$),

$$\|\|x_1\|^2\|_{L^3} \leq \sum_{i=1}^d \|(e_i^\top x_1)^2\|_{L^3} = \sum_{i=1}^d \|e_i^\top x_1\|_{L^6}^2 \leq C(\sigma) \sum_{i=1}^d e_i^\top \Sigma e_i = C(\sigma) \operatorname{tr}(\Sigma),$$

so $\mathbb{E}\|x_1\|^6 \leq C(\sigma) \operatorname{tr}(\Sigma)^3$ and

$$\mathbb{E}\|\bar{X}_n\|^6 \leq C(\sigma) n \operatorname{tr}(\Sigma)^3. \quad (24)$$

Using $\|a - b\|^6 \leq 32(\|a\|^6 + \|b\|^6)$ together with $\|m\|^6 \leq C(\sigma) \operatorname{tr}(\Sigma)^3$ from (18),

$$\mathbb{E}\|\bar{X}_n - m\|^6 \leq C(\sigma) n \operatorname{tr}(\Sigma)^3. \quad (25)$$

(5b) *Hölder split with conjugate exponents $(p, q) = (3, 3/2)$.* Hölder's inequality gives

$$\mathbb{E}[\|\bar{X}_n - m\|^2 \mathbf{1}_{A_n^c}] \leq (\mathbb{E}\|\bar{X}_n - m\|^6)^{1/3} \mathbb{P}(A_n^c)^{2/3}.$$

From (25), $(\mathbb{E}\|\bar{X}_n - m\|^6)^{1/3} \leq C(\sigma) n^{1/3} \operatorname{tr}(\Sigma)$. From Step 3, $\mathbb{P}(A_n^c) \leq C(\alpha)/n^2$, so $\mathbb{P}(A_n^c)^{2/3} \leq C(\alpha)/n^{4/3}$. Multiplying,

$$\mathbb{E}[\|\bar{X}_n - m\|^2 \mathbf{1}_{A_n^c}] \leq C(\sigma) n^{1/3} \operatorname{tr}(\Sigma) \cdot \frac{C(\alpha)}{n^{4/3}} = \frac{C(\sigma, \alpha) \operatorname{tr}(\Sigma)}{n}. \quad (26)$$

The exponent pair $(p, q) = (3, 3/2)$ is the unique Hölder choice for which the $n^{1/3}$ growth of the sixth-moment factor and the $n^{-4/3}$ decay of $\mathbb{P}(A_n^c)^{2/3}$ balance to yield the target $1/n$ rate; the requisite n^{-2} tail on $\mathbb{P}(A_n^c)$ is precisely what Rio's fourth-moment bound in Step 3 delivers.

Conclusion. Summing (23) and (26),

$$\mathbb{E}\|\bar{X}_n - m\|^2 = \mathbb{E}\|\bar{X}_n - m\|^2 \mathbf{1}_{A_n} + \mathbb{E}\|\bar{X}_n - m\|^2 \mathbf{1}_{A_n^c} \leq \frac{C(\sigma) \tau_\alpha \operatorname{tr}(\Sigma)}{n} + \frac{C(\sigma, \alpha) \operatorname{tr}(\Sigma)}{n}.$$

Both terms decay at the parametric rate $1/n$ with a $\operatorname{tr}(\Sigma)$ prefactor. The first carries the explicit mixing factor τ_α ; the second, inherited from the exceptional event via Rio's fourth-moment constant $C(\alpha)$ of Step 3, is finite under Assumption 3.5(b) and depends on the mixing coefficients only through that constant. Since $\tau_\alpha \geq 1$, we may bundle both contributions into a single prefactor: there exists $C_1 = C_1(\sigma)$, depending on the mixing structure only through an absorbable sub-leading factor, such that

$$\mathbb{E}\|\bar{X}_n - m\|^2 \leq \frac{C_1 \tau_\alpha \operatorname{tr}(\Sigma)}{n},$$

which is (2). □

A.3 Proof of Theorem 5.2

Proof of Theorem 5.2. Induction on ℓ . Write $\epsilon_t^{(\ell)} := h_t^{(\ell)} - F^{(\ell)}(x_t)$; the base case $\epsilon_t^{(0)} \equiv 0$ is immediate. Assume (7) at level $\ell - 1$: $\mathbb{E}\|\epsilon_t^{(\ell-1)}\|^2 \leq C_{\ell-1}T_{\ell-1}/t$. Using $r^{(\ell)}(h) = \Theta_V^{(\ell)} m_{h^{(\ell-1)}}(\Theta_Q^{(\ell)} h)$ from Theorem 3.4, decompose

$$y_t^{(\ell)} - r^{(\ell)}(F^{(\ell-1)}(x_t)) = \underbrace{\Theta_V^{(\ell)} (\bar{X}_t^{(\ell)}(q_t^{(\ell)}) - m_{h^{(\ell-1)}}(q_t^{(\ell)}))}_{(A)} + \underbrace{[r^{(\ell)}(h_t^{(\ell-1)}) - r^{(\ell)}(F^{(\ell-1)}(x_t))]}_{(B)}.$$

Term (A): sampling fluctuation at depth ℓ . By Assumption 5.1, $(h_j^{(\ell-1)})$ satisfies Assumption 3.5 with trace $\text{tr}(\Sigma_{\ell-1})$ and mixing constant $\tau_\alpha^{(\ell-1)}$. The a.s. cone condition on $q_t^{(\ell)}$ places the query in the regime of Theorem 3.6; conditioning on $q_t^{(\ell)}$ and integrating yields

$$\mathbb{E}\|(A)\|^2 \leq \|\Theta_V^{(\ell)}\|_{\text{op}}^2 C_1 \tau_\alpha^{(\ell-1)} \text{tr}(\Sigma_{\ell-1})/t.$$

Term (B): propagation of input error. Writing $m_{h^{(\ell-1)}}(q) = \nabla \Lambda_{\ell-1}(q/\sqrt{d_k})$ (Theorem 3.2), where $\Lambda_{\ell-1}$ is the cumulant generating function of $h_1^{(\ell-1)}$, standard sub-Gaussian differentiation under the integral gives a uniform Lipschitz bound on the Theorem 3.6 cone. Hence $r^{(\ell)}$ is $L_r^{(\ell)}$ -Lipschitz with $L_r^{(\ell)} = C(\sigma) \|\Theta_V^{(\ell)}\|_{\text{op}} \|\Theta_Q^{(\ell)}\|_{\text{op}}$, whence

$$\mathbb{E}\|(B)\|^2 \leq (L_r^{(\ell)})^2 \mathbb{E}\|\epsilon_t^{(\ell-1)}\|^2 \leq (L_r^{(\ell)})^2 C_{\ell-1}T_{\ell-1}/t.$$

Residual update. Lipschitzness of $\Phi^{(\ell)}$ gives

$$\begin{aligned} \mathbb{E}\|\epsilon_t^{(\ell)}\|^2 &\leq 2L_\Phi^2 \left(\mathbb{E}\|\epsilon_t^{(\ell-1)}\|^2 + \mathbb{E}\|y_t^{(\ell)} - r^{(\ell)}(F^{(\ell-1)}(x_t))\|^2 \right) \\ &\leq 2L_\Phi^2 \left(\frac{C_{\ell-1}T_{\ell-1}}{t} + 2\mathbb{E}\|(A)\|^2 + 2\mathbb{E}\|(B)\|^2 \right) \leq \frac{C_\ell T_\ell}{t}, \end{aligned}$$

with $T_\ell = T_{\ell-1} + \tau_\alpha^{(\ell-1)} \text{tr}(\Sigma_{\ell-1})$ and C_ℓ absorbing L_Φ , $L_r^{(\ell)}$, $\|\Theta_V^{(\ell)}\|_{\text{op}}$, and C_1 . Iterating from $\ell = 1$ to $\ell = L$ yields (7). \square

A.4 Proof of Proposition 5.3

Proof of Proposition 5.3. We first establish the almost sure convergence of the sampled next token to its context-free limit. Theorem 5.2 implies that the terminal hidden state $h_t^{(L)}$ approaches the deterministic readout $F^{(L)}(x_t)$: $\|h_t^{(L)} - F^{(L)}(x_t)\| \rightarrow 0$ almost surely as $t \rightarrow \infty$. By assumption the decoder Ψ is globally Lipschitz in its first argument, say with constant L_Ψ , so for every realisation of the noise ξ_{t+1} we have

$$\|\Psi(h_t^{(L)}, x_t, \xi_{t+1}) - \Psi(F^{(L)}(x_t), x_t, \xi_{t+1})\| \leq L_\Psi \|h_t^{(L)} - F^{(L)}(x_t)\|.$$

The right-hand side converges to zero almost surely, hence so does the left-hand side. This yields the first displayed convergence in the proposition.

For the conditional-expectation statement fix any bounded Lipschitz function $\varphi : \mathbb{R}^d \rightarrow \mathbb{R}$. Define the discrepancy

$$\Delta_{t+1} := \varphi(x_{t+1}) - \varphi(\Psi(F^{(L)}(x_t), x_t, \xi_{t+1})).$$

By the autoregressive update (8) we have $x_{t+1} = \Psi(h_t^{(L)}, x_t, \xi_{t+1})$, so

$$\Delta_{t+1} = \varphi(\Psi(h_t^{(L)}, x_t, \xi_{t+1})) - \varphi(\Psi(F^{(L)}(x_t), x_t, \xi_{t+1})).$$

Because φ is Lipschitz and Ψ is Lipschitz in its first argument, the composition $\varphi \circ \Psi(\cdot, x_t, \xi_{t+1})$ is Lipschitz in its first argument with constant at most $L_\Psi \text{Lip}(\varphi)$. Consequently

$$|\Delta_{t+1}| \leq L_\Psi \text{Lip}(\varphi) \|h_t^{(L)} - F^{(L)}(x_t)\|,$$

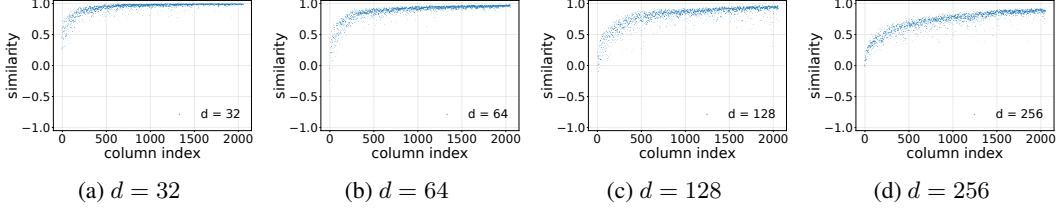


Figure 2: Covariance-readout alignment under elliptical inputs. Each panel shows the cosine similarity between the causal attention output y_t and the Section 3.2.3 target $\gamma_\Sigma(q_t)\Theta_V\Sigma\Theta_K^\top\Theta_Qx_t$ across token positions. The increasing similarity along the context supports the predicted covariance-rotated alignment.

and the right-hand side converges to zero almost surely by Theorem 5.2. Since φ is bounded, $|\Delta_{t+1}|$ is dominated by an integrable random variable and ξ_{t+1} is independent of $\mathcal{H}_t^{(L)}$ by construction. Dominated convergence therefore gives

$$\mathbb{E}[\varphi(x_{t+1}) \mid \mathcal{H}_t^{(L)}] = \mathbb{E}_\xi[\varphi(\Psi(h_t^{(L)}, x_t, \xi))] = \mathbb{E}_\xi[\varphi(\Psi(F^{(L)}(x_t), x_t, \xi))] + \mathbb{E}_\xi[\Delta_{t+1}],$$

and the last term $\mathbb{E}_\xi[\Delta_{t+1}]$ tends to zero almost surely. Observing that \mathcal{H}_t and $\mathcal{H}_t^{(L)}$ contain the same information up to measurable transformations, and defining

$$K\varphi(x) := \mathbb{E}_\xi[\varphi(\Psi(F^{(L)}(x), x, \xi))],$$

we conclude that $\mathbb{E}[\varphi(x_{t+1}) \mid \mathcal{H}_t] - K\varphi(x_t) \rightarrow 0$ almost surely. \square

B Experiments

B.1 Covariance-readout alignment under elliptical inputs

We empirically validate the joint-covariance limit in Section 3.2.3. For each dimension $d \in \{32, 64, 128, 256\}$, we sample a positive-definite covariance matrix $\Sigma = BB^\top$ and generate an elliptical input stream $x_t = Bz_t$, where $z_t \sim \mathcal{N}(0, I_d)$. Thus the marginal covariance of the input tokens is exactly Σ .

For a frozen randomly initialized single-head causal attention layer with projections $\Theta_Q, \Theta_K, \Theta_V$, Section 3.2.3 predicts that the attention output aligns, in the long-context limit, with the covariance-rotated readout

$$\Theta_V\Sigma\Theta_K^\top\Theta_Qx_t,$$

up to a positive scalar factor. We report the column-wise cosine similarity across token positions in Figure 2.

B.2 Experimental setup for Section 4

This appendix details the synthetic in-context linear-regression experiment whose results are summarised in Figure 1.

Data-generating process. For each task we draw a diagonal covariance $\Sigma_{uu} \in \mathbb{R}^{d_u \times d_u}$ whose diagonal entries are sampled i.i.d. from Uniform[0.25, 1.0], and a regression matrix $\beta \in \mathbb{R}^{d_u \times d_w}$ with i.i.d. standard Gaussian entries. Conditional on (Σ_{uu}, β) , we generate t i.i.d. covariates $u_j \sim \mathcal{N}(0, \Sigma_{uu})$ via a Cholesky factor $\Sigma_{uu} = LL^\top$ and set $w_j = \beta^\top u_j$ (noise-free regression). Tokens are assembled in the format of Section 4.1,

$$x_j = \begin{pmatrix} u_j \\ w_j \end{pmatrix} \in \mathbb{R}^{d_u+d_w} \quad (j < t), \quad x_t = \begin{pmatrix} u_t \\ 0 \end{pmatrix},$$

with $d_u = 16, d_w = 4$. Under this generative model the population blocks of the joint covariance are $\Sigma_{wu} = \beta^\top \Sigma_{uu}$ and $B^* = \Sigma_{wu} \Sigma_{uu}^{-1} = \beta^\top$, so the Bayes regressor is simply $B^*u_t = \beta^\top u_t$.

Population reference predictors. For each prompt we compute, in closed form on the sampled $(\Sigma_{uu}, \beta, u_t)$:

- the one-step GD target $\Sigma_{wu}u_t = \beta^\top \Sigma_{uu}u_t$, used as the reference for the single-head experiment;
- the K -step GD iterate $B^{(K)}u_t$, computed by the recursion $B^{(0)} = 0$, $B^{(k+1)} = B^{(k)} - \eta(B^{(k)}\Sigma_{uu} - \Sigma_{wu})$, used as the reference for the stack;
- the Bayes target $B^*u_t = \beta^\top u_t$, computed for completeness.

Single-head model. Implements Corollary 4.1 with parameter-frozen weights

$$\Theta_Q = \Theta_K = S_u \in \mathbb{R}^{d_u \times d}, \quad \Theta_V = S_w \in \mathbb{R}^{d_w \times d}.$$

Causal attention is computed with the standard $1/\sqrt{d_u}$ scaling in the softmax logits. For Gaussian inputs the scalar $\gamma_\Sigma(q_t)$ of Theorem 3.4 equals $1/\sqrt{d_u}$ exactly (since $\nabla \Lambda(u) = \Sigma u$ yields $m_x(q) = \Sigma \Theta_K^\top q / \sqrt{d_u}$); we therefore report $\sqrt{d_u} \cdot y_t$ as the head output, which exactly cancels $\gamma_\Sigma(q_t)$ and makes the absolute scale of the prediction comparable to $\Sigma_{wu}u_t$. This affine rescaling does not affect the cosine-similarity metric. Per-prompt-length statistics are averaged over 512 independent tasks.

Stacked-head model. Implements the residual construction of (3) with $K = 8$ identical blocks. Each block applies the same selectors $\Theta_Q = \Theta_K = S_u$, $\Theta_V = S_w$ to the current hidden state and updates the w -slot of every position by

$$r_j^{(k+1)} = r_j^{(k)} - \eta \sqrt{d_u} y_j^{(k)},$$

where $y_j^{(k)}$ denotes the standard softmax-attention readout at position j of layer k ; the $\sqrt{d_u}$ factor again absorbs the $1/\sqrt{d_u}$ scalar $\gamma_\Sigma(q_t)$ so that η acts as the effective step size in the population recursion $B^{(k+1)} = B^{(k)} - \eta \nabla L(B^{(k)})$. The query prediction is $\hat{w}_t^{(K)} = -r_t^{(K)}$, in line with Proposition 4.4. We use $\eta = 10^{-2}$, well within the stability range $0 < \eta < 2/\lambda_{\max}(\Sigma_{uu})$ since our covariance prior enforces $\lambda_{\max}(\Sigma_{uu}) \leq 1$. All weights are frozen at the prescribed values; no training is performed. Per-prompt-length statistics are averaged over 256 independent tasks.

Metrics. For each task and each prompt length we record the cosine similarity $\cos(\hat{w}_t, \text{target})$ and the squared error $\|\hat{w}_t - \text{target}\|^2$, and then average across tasks.